AUTOINDUCER-2 QUORUM SENSING REGULATION OF BACTERIAL COLONIZATION AND POPULATION DISTRIBUTION IN THE ZEBRAFISH INTESTINE

by

MARIA SOLEDAD BAÑUELOS

A DISSERTATION

Presented to the Department of Biology
and the Graduate School of the University of Oregon
in partial fulfillment of the requirements
for the degree of
Doctor of Philosophy

September 2020

DISSERTATION APPROVAL PAGE

Student: Maria Soledad Bañuelos

Title: Autoinducer-2 Quorum Sensing Regulation of Bacterial Colonization and Population Distribution in the Zebrafish Intestine

This dissertation has been accepted and approved in partial fulfillment of the requirements for the Doctor of Philosophy degree in the Department of Biology by:

Brendan Bohannan	Chairperson
Karen Guillemin	Advisor
Michael Harms	Core Member
Anne Zemper	Core Member
Tristan Ursell	Institutional Representative

and

Kate Mondloch	Interim Vice Provost and Dean of the Graduate School

Original approval signatures are on file with the University of Oregon Graduate School.

Degree awarded September 2020.

DISSERTATION ABSTRACT

Maria Soledad Bañuelos

Doctor of Philosophy

Department of Biology

September 2020

Title: Autoinducer-2 Quorum Sensing Regulation of Bacterial Colonization and Population Distribution in the Zebrafish Intestine

Quorum sensing is a mode of bacterial communication that relies on the production and secretion of signaling molecules known as autoinducers. Group-wide detection of autoinducers gives rise to collective gene expression patterns that make coordinated group behaviors possible. Behaviors vary across bacterial species but often include: secretion of virulence factors, changes in motility, and biofilm formation. While many autoinducers exhibit high specificity and are used to foster intraspecies communication, one molecule known as Autoinducer-2 (AI-2) is produced and detected by numerous bacterial species. Interestingly, while AI-2 is known to mediate aggregation and biofilm formation of bacteria through the traditional gene regulatory mechanisms, it uniquely can also do so through the use of chemotaxis signaling. For example, *Helicobacter pylori* perceives AI-2 as a chemorepellent and in turn this chemorepulsion response results in cell dispersal from biofilms. Conversely, in *Escherichia coli* AI-2 induces cell aggregation via gene expression changes and by serving as a chemoattractant that recruits cells to aggregates. Currently much of the research involving AI-2 has been carried out in monoculture *in vitro* biofilms and has focused on the role of AI-2 as a mediator of biofilm formation and biofilm membership. Here we investigate the role of

AI-2 in colonization and spatial distribution of bacterial communities inside an animal host. To address this we colonized larval zebrafish with wild type *E. coli*, an AI-2 synthesis mutant *ΔluxS*, or an AI-2 signaling mutant *ΔlsrR*. We then used a combination of plate based assays and live imaging to determine the abundance and spatial distribution of the gut bacteria. We observed that in a mono-association, *E. coli* mutants lacking the ability to produce or detect AI-2 showed increased intestinal abundance. Additionally, we observed differing spatial localizations between populations of *ΔluxS* bacteria that had been untreated or treated with AI-2. Populations exposed to AI-2 localized more distally along the axis of the intestine, consistent with increased displacement. Further, we showed that native gut bacteria of the zebrafish exhibit analogous responses to AI-2, indicating that interspecies AI-2 signaling could play an important role in microbiome composition and biogeography.

This dissertation includes previously unpublished co-authored material.

CURRICULUM VITAE

NAME OF AUTHOR: Maria Soledad Bañuelos

GRADUATE AND UNDERGRADUATE SCHOOLS ATTENDED:

University of Oregon, Eugene OR
University of Redlands, Redlands CA

DEGREES AWARDED:

Doctor of Philosophy, Biology, 2020, University of Oregon
Bachelor of Science, Molecular Biology and Biochemistry, 2014, University of Redlands

AREAS OF SPECIAL INTEREST:

Microbiology

PROFESSIONAL EXPERIENCE:

Graduate Teaching Assistant, University of Oregon, September 2014 - June 2015

Undergraduate Lab Assistant, University of Redlands, September 2012 - April 2013

Biology Tutor, University of Redlands, September 2010 - April 2014

GRANTS, AWARDS, AND HONORS:

NIH Training Grant in Molecular Biology and Biophysics (7T32GM007759-37), University of Oregon, 2015-2016

Phi Beta Kappa scholarship for graduate studies, University of Redlands, 2014

PUBLICATIONS:

Banuelos, M.S., Schlomann, B.H., Pokorny, C., Parthasarathy, R., Guillemin, K. Autoinducer-2 quorum sensing reduces gut bacterial abundance and alters spatial distribution. *In preparation*.

Sweeney, E.G., Nishida A., Weston A., **Bañuelos M.S.**, Potter K., Conery J., Guillemin K. (2019). Agent-based modeling demonstrates how local chemotactic behavior can shape biofilm architecture. mSphere 4:e00285-19.

Grimley, S.J, Ko, M.O., Morrell, H.E.R., Grace, F., **Bañuelos, M.S.,** Bautista, B.R., Chavez, G.N., Huerta, M., Marks, M., Ov, J., Overton-Harris, P., Olson, L.E. (2018). The need for a neutral speaking period in psychosocial stress testing. Journal of Psychophysiology 2019 33:4, 267-275.

Bañuelos, M. S., Musleh, A., Olson, L. E. (2017). Measuring Salivary Alpha-Amylase in the Undergraduate Neuroscience Laboratory. Journal of undergraduate neuroscience education: JUNE: a publication of FUN, Faculty for Undergraduate Neuroscience, 16(1), A23–A27.

ACKNOWLEDGMENTS

I would like to express my appreciation for my mentor, Dr. Karen Guillemin. This work would not exist without her guidance, encouragement, and patience. She is quite a talented and empathetic leader and I could not have picked a better mentor. Thank you Karen for your enduring support. I would also like to thank the members of my advisory committee – Brendan Bohannan, Michael Harms, Tristan Ursell, and Anne Zemper – for their valuable input on my research and for their continuous encouragement during difficult times. Additionally I would like to express gratitude to my colleagues in the Guillemin, Eisen, and Parthasarathy labs who graciously shared their expertise and insight. Specifically, Dr. Emily Sweeney and Dr. Travis Wiles who mentored me throughout my time as a graduate student and were always available for meaningful discussions. Thank you to Elena Wall and Michelle Massaquoi for the conversations about science and non-science topics and for the laughs that often followed.

I would also like to thank all my collaborators including undergraduate, Claire Pokorny, who provided technical assistance for the work presented in Chapter II and III, Dr. Brandon Schlomann for assistance in collecting imaging data for the work presented in Chapter II, and Dr. Parthasarathy for providing valuable input on the direction of the project and on the statistical methods used in Chapter II.

I am grateful to my good friends Aleesa Schlientz and Emily Sutton who took this journey with me. Thank you gals for the friendship and support throughout these six years. I owe a good amount of my successes to your support.

Finally, I would like to acknowledge my family. Thank you mom and dad for always expressing your pride in my achievements even when I struggled to see them as such. To my brothers and sisters I thank you for lifting my spirits by believing in me when I did not believe in myself and thank you for quickly grounding me with your lighthearted teasing. Lastly, I could not go without mentioning my niece and nephews who often served as my motivation to push through challenging moments. I am excited to keep sharing milestones with you.

This dissertation is dedicated to my family and friends for their unending love and support.

TABLE OF CONTENTS

LIST OF FIGURES

Figure Page

CHAPTER I

INTRODUCTION

Quorum Sensing: Communication in the bacterial world

For many years it was believed that bacteria functioned solely as individual organisms that competed with one another for resources. It was not until the 1970's that evidence suggestive of bacterial collective behaviors came to light. In a seminal paper, Nealson et al. reported that *Vibrio fischeri* produced extracellular molecules that induced population-wide luminescence (1). While at first this was thought to be a unique trait to *V. fischeri,* by the 1990's the idea of bacterial cell communication and group behaviors was widely accepted as true for many bacterial species. This method of bacterial cell-to-cell communication would be coined quorum sensing (QS)(2).

QS is a type of bacterial cell signaling mechanism that involves the production, secretion, and detection of small molecules known as autoinducers. Autoinducers accumulate in the local environment in a cell density dependent manner and are detected via autoinducer specific receptors (3–9). Group-wide detection of autoinducers results in altered global gene expression patterns that trigger collective behaviors such as bioluminescence, the production of public goods, the secretion of virulence factors, changes in motility, and biofilm formation (5–19).While these behaviors can be costly for individual cells, they become effective when performed by the entire population (2, 8, 20)

Fostering interspecies communication with Autoinducer-2

Several autoinducers have now been identified and grouped into two broad categories: small peptides produced by Gram positive bacteria and Acyl-Homoserine Lactones (AHLs) produced by Gram negative bacteria (2–9). These QS signals are often species or genus specific, promoting intraspecies communication (2–9). However, one autoinducer, known as Autoinducer-2 (AI-2), falls outside of these two categories and is shared by both Gram positive and Gram negative species (6, 12, 25). AI-2 is a furanol diester that is produced by the enzyme LuxS as a byproduct of the activated methyl cycle (6, 12, 25). The *luxS* gene is found in over 500 species of bacteria, suggesting that AI-2 production is extremely common (26). Due to its ubiquitous nature, AI-2 has been suggested to foster interspecies communication (6, 12, 25, 26).

Interestingly, while AI-2 is produced by a variety of bacterial species, the receptors for AI-2 and the collective behaviors mediated by AI-2 differ across species. To date, four unique AI-2 binding proteins have been identified one in *Vibrio harveyi,* one in *Escherichia coli,* and two in *Helicobacter pylori* (27–29). These three bacteria also display unique responses to the AI-2 molecule. In *V. harveyi* AI-2 induces luminescence, in *E. coli* it serves as a chemotactic cue and induces biofilm formation, and in *H. pylori* it serves as a chemotactic cue that promotes biofilm dispersal (27–29). It is important to note that while only four AI-2 binding proteins have been identified, AI-2 has been shown to elicit QS behaviors in a much larger number of species (19, 30–35).

The effects of AI-2 QS on host-associated community composition

As our knowledge about the molecular mechanisms underlying QS expands, we are shifting our interests to understanding the role of QS in the context of host associated microbial communities. Evidence suggesting that AI-2 QS modulates host-associated community composition is limited but is none the less striking. Work done in the Gordon lab showed that after co-colonizing gnotobiotic mice with *Vibrio cholerae* and a community of human species, a human isolate of *Ruminococcus obeum* restricted colonization of *V. cholerae* and did so by increasing its own production of AI-2 (36). *R. obeum* AI-2 was then shown to cause QS mediated repression of several *V. cholerae* genes (36). Further, work done by the Xavier lab showed that altering AI-2 concentrations in the mouse gut resulted in changes in the microbial community composition (37). In this case, the authors gave mice a treatment of antibiotics and found that this induced dysbiosis of the mouse intestinal community, nearly clearing out the *Firmicutes.* However upon colonization with *E. coli* strains that were engineered to increase intestinal AI-2 concentrations, expansion of *Firmicutes* was observed (37). These studies demonstrate that AI-2 QS in the vertebrate intestine can alter community composition through both intraspecies and interspecies interactions.

While these examples demonstrate AI-2 mediated bacterial community composition shifts, the mechanism by which AI-2 regulated bacterial behaviors to alter colonization and membership have not been elucidated. In fact, the majority of AI-2 QS research does not focus on composition changes but rather on revealing the mechanisms by which AI-2 mediates *in vitro* biofilm formation and spatial structure. AI-2 has been

shown to regulate biofilm formation in a number of diverse organisms such as *Escherichia, Helicobacter, Bacillus, Streptococcus, Aggregatibacter, Pseudomonas, Staphylococcus,* and *Klebsiella* (18, 19, 27, 31–34, 38, 39). Work done in the Guillemin lab investigated the role of AI-2 in *H. pylori* biofilm formation and found that AI-2 results in dispersal from biofilms (27). They further elucidated the mechanism governing this behavior and discovered that *H. pylori* perceives AI-2 as a chemotactic cue that the bacteria swim away from (17, 27, 40). In a high cell density community such as a biofilm, where AI-2 accumulates to higher concentrations, cells experience chemorepulsion from AI-2, ultimately causing them to leave the biofilm (17, 27, 40). Cells unable to chemotax away from AI-2 produced larger biofilms with a more homogenous organization of bacterial cell clusters (27). Agent-based modeling was then used to simulate *H. pylori* biofilm growth of strains with varying AI-2 producing and sensing capabilities (40). The simulations recapitulated the previous observations and provided a more detailed view of the biofilm structures (40). Ultimately the modeling supported the idea that cells that dispersed from biofilms due to chemorepulsion from AI-2 formed smaller and more heterogeneously spaced biofilms, whereas cells that were defective for AI-2 chemotaxis produced larger and more evenly spaced structures (27, 40). While this example of how AI-2 signaling mediates biofilm formation and structure may seem disconnected to the mechanisms by which AI-2 influences host-associated microbial composition, it is important to recognize the role of biofilm formation as analogous to aggregate formation. Although there is debate in the field about whether biofilms and bacterial aggregates are one in the same, ultimately both are cell clusters

that have the capacity to be sources of AI-2. To further expand on this connection, in the following section I will review the key features connecting aggregation to host microbiota community composition and biogeography.

Bacterial cohesion in the zebrafish intestine

In an effort to characterize the behavior of the zebrafish resident microbiota, the Guillemin and Parthasarathy labs conducted a high-resolution comparative study of bacterial distribution patterns throughout the intestine of live, larval zebrafish (41). The bacterial symbionts that were used showed large differences in cohesion (the degree to which they aggregate) and spatial distribution (41). The study revealed a striking correlation between each strain's position along the intestine and its cohesive properties within the intestine. Those strains that experienced more aggregation tended to localize in the distal regions of the intestine (41). Strains that experienced less aggregation and thus had more planktonic individuals in the population, tended to localize to the anterior regions of the intestine (41). The strong correlation between the cohesive nature of strains and their localization along the gut illustrated the generality of the role of cohesion in the stability of bacterial populations in the intestine. In depth analysis of certain bacterial strains with live imaging demonstrated that the larval zebrafish intestine undergoes peristalsis-like movements that result in the expulsion of bacterial communities (41–44). Bacteria that are highly clustered experience these peristaltic contractions more acutely and are displaced in the distal intestine. Here they are subject to more expulsion events as these peristaltic movements are amplified in the distal portion of the intestine (41–44).

These expulsion events, depending on the cohesive nature of the bacteria, can result in the expulsion of up to ~90% of the population (41–44). The continuous movement of the intestinal walls means that all bacteria experience expulsion events and it is the remaining planktonic cells that go on to repopulate the intestine by proliferating. However, for those populations that are highly aggregated, an expulsion event can result in complete extinction from the intestine (42, 43). This was shown in a subsequent study where zebrafish were singly colonized by highly aggregated *Enterobacter* or highly planktonic *Vibrio* and treated with antibiotics (42). While the antibiotics were shown to induce aggregation in both strains, increased aggregation of *Enterobacter,* which started off highly clustered, resulted in depletion of all planktonic cells. When *Enterobacter* was then expelled from the intestine, there were no remaining cells to repopulate, leading to the disappearance of *Enterobacter* from the intestine (42).

In a separate study, the impact of bacterial cohesion was investigated in the context of competition between two bacterial species in the intestine (43). In this study, larval zebrafish were colonized with a single, highly aggregated strain of *Aeromonas*, or were colonized by a two species community consisting of *Aeromonas* and a highly planktonic strain of *Vibrio* (43). When *Aeromonas* was on its own, it experienced expulsion events but was able to repopulate the intestine. Interestingly, when invaded with *Vibrio*, the *Aeromonas* was unable to repopulate (43). This same experiment was carried out in zebrafish that exhibited reduced peristalsis due to a mutation in the ret gene, and in this case *Aeromonas* was able to persist in the presence of *Vibrio* (43). This work suggests that the inherent cohesiveness of the bacterial population in conjunction

with host intestinal movements can have a large impact on the composition and spatial distribution of the microbiota. These findings motivate the hypothesis that factors that govern bacterial aggregation, such as AI-2, are likely to impact the composition and spatial distribution of bacterial communities within the intestine. Therefore, in a first study of AI-2 impacts on bacterial population spatial dynamics *in vivo*, I will use the larval zebrafish system to investigate a role for AI-2 QS in host colonization and determine the role of AI-2 mediated cohesion on the spatial distribution of bacterial populations in the intestine.

Bridge

In the following chapters of my dissertation I will discuss my efforts to determine the role of AI-2 QS in host colonization and bacterial spatial distribution. Chapter II will center on my work using the larval zebrafish model to demonstrate that AI-2 QS results in distal displacement of bacterial populations and leads to reduced intestinal colonization levels. From this work, I identified two closely related *Vibrio* species that carry the same AI-2 QS receptors and associated genes yet display different phenotypes when exposed to AI-2. Chapter III will discuss a bioinformatic approach I took to explain why these two *Vibrio* isolates differ in AI-2 responses despite carrying the same AI-2 QS gene network. Finally, in chapter IV I will put my work into the larger context of the impacts of AI-2 QS on the composition of multispecies bacterial communities.

Chapters II and III contain co-authored, unpublished material by myself and collaborators: Dr. Brandon Schlomann (Parthasarathy Lab, University of Oregon) who

performed the light sheet fluorescence microscopy imaging in chapter II and Claire Pokorny (Guillemin lab, University of Oregon) who helped generate genetic tools, performed gut dissections, and carried out *Vibrio* sequence alignments for chapters II and III.

CHAPTER II

AUTOINDUCER-2 SIGNALING ALTERS INTESTINAL COLONIZATION AND SPATIAL DISTRIBUTION OF BACTERIAL COMMUNITIES IN THE ZEBRAFISH INTESTINE

This chapter contains unpublished, co-authored material. Brandon Schlomman (Parthasarathy Lab, University of Oregon) collected the light sheet imaging data and assembled Figure 2 panels A-C and Figure 3 panel A. Claire Pokorny (Guillemin Lab, University of Oregon) aided in data collection for Figures 1, 3 and 4.

Introduction

Quorum sensing (QS) is a form of bacterial cell communication by which bacteria coordinate group-wide behaviors in response to changes in cell density (1-8). QS involves the cellular production, secretion, and detection of small signaling molecules known as autoinducers (1-8). Detection of autoinducers leads to altered gene expression patterns that give rise to population-wide behaviors (1–8). QS can regulate an expansive set of behaviors including bioluminescence, motility, virulence factor production, and biofilm formation (2, 4–8).

Many QS signals are species or genus specific, allowing only intraspecies communication to take place. However, one molecule known as Autoinducer-2 (AI-2) is thought to foster interspecies communication due to its prevalence in both Gram positive

and Gram negative bacterial species (6–8, 25, 45). AI-2 has been implicated in aggregation and biofilm formation in a wide variety of bacterial species such as *Escherichia, Helicobacter, Bacillus, Streptococcus, Aggregatibacter, Pseudomonas, Staphylococcus,* and *Klebsiella* (11, 18, 19, 27, 30–35, 39). In the case of *Escherichia coli* AI-2 has been shown to induce aggregation both via changes in gene expression patterns and as a chemoattractant that recruits cells to aggregates (11, 18, 28, 46, 47). In contrast, *Helicobacter pylori* perceives AI-2 as a chemorepellent and in turn this chemorepulsion causes cells to disperse from biofilms (17, 27, 40). The widespread nature of AI-2 However, much of the research involving AI-2 has been carried out in monoculture *in vitro* biofilms and has not addressed the role of AI-2 as a mediator of multi-species behaviors in host-associated microbial communities.

A few studies suggest a role for AI-2 QS in multispecies host colonization. For example, the Gordon lab showed that co-colonizing gnotobiotic mice with *Vibrio cholerae* and a community of human bacterial species, restricted colonization of *V. cholerae* (36). This was shown to be dependent on AI-2 production by a *Ruminococcus obeum* isolate from humans, which resulted in QS mediated repression of *V. cholerae* genes (36). Further, in work done by the Xavier lab, mice were treated with antibiotics to induce dysbiosis of the mouse intestinal community resulting in a dramatic reduction of the Firmicutes (37). The mice were then colonized with *E. coli* strains that were engineered to increase intestinal AI-2 concentrations resulting in recovery of Firmicutes (37). This showed that altering AI-2 concentrations in the mouse gut results in changes to bacterial community composition.

While these studies demonstrate that AI-2 QS in the vertebrate intestine can alter community composition, they fail to provide a mechanistic understanding of how the cellular behavior regulated by AI-2 results in altered colonization. Research in gnotobiotic larval zebrafish has demonstrated how the bacterial cellular response of increased cohesion can result in bacterial community changes in colonization by altering how the bacterial community experiences gut motility, with more aggregated populations being more readily displaced (41–44). Therefore, we decided to use the zebrafish gut ecosystem to investigate the role of AI-2 signaling in intestinal colonization and structuring of bacterial communities residing in the vertebrate gut. Here we predominantly work with *E. coli* due to the fact that it has a well characterized AI-2 signaling pathway and can effectively colonize the larval zebrafish intestine (11, 28, 47, 48).

We observed that disruption of *E. coli* AI-2 sensing leads to increased intestinal colonization. We also observed that treating *E. coli* communities already residing in the gut with exogenous AI-2 leads to a drop in their abundance. We further show that native gut bacteria of the zebrafish exhibit analogous responses to AI-2, suggesting that inter-species AI-2 signaling could play an important role in microbiome composition and biogeography in the vertebrate intestine.

Results

AI-2 signaling decreases intestinal abundance of *E. coli*

To investigate the role of AI-2 QS during intestinal colonization we generated *E. coli* single gene knockouts of AI-2 synthase gene *luxS* and the AI-2 transcriptional regulation gene *lsrR*. The Δ*luxS* mutant lacks AI-2 production, but this strain should still be responsive to AI-2 provided from other bacteria or AI-2 added exogenously. The Δ*lsrR* mutant should be blind to AI-2 and is also expected to act as an AI-2 sink due to the fact that in the absence of LsrR, cells increase production of AI-2 uptake machinery (49). To confirm that our mutants behaved as previously reported in the literature, we measured the AI-2 activity in their cell free supernatant that induced luminescence in a *Vibrio harveyi* reporter strain (50). All measurements were normalized to the AI-2 activity in the cell free supernatant from the wild type *E. coli* strain (Fig1A). As expected, the Δ*luxS* strain lacked appreciable AI-2 activity. We were able to restore this activity by complementation of the gene *(*Δ*luxS*+). AI-2 activity of Δ*lsrR* was significantly reduced, consistent with previous reports that Δ*lsrR* strains scavenge environmental AI-2 (Fig1A) (49). We also generated an AI-2 over producer strain (*luxS*$^{OP)}$ with an extra copy of *luxS* and confirmed that this strain produced increased AI-2 activity. To assess if disruption of AI-2 signaling plays a role in host colonization we inoculated the water column of germ free larval zebrafish with either wild type *E. coli*, Δ*luxS*, Δ*lsrR*, Δ*luxS*+*,* or *luxS*^{OP} at 4 days post fertilization (dpf), when the larval gut is patent and accessible to environmental microbes. Following 72 hours post inoculation, which provides ample time for bacteria to colonize, proliferate, and reach a climax community (48, 51), we dissected the intestines

of the mono-associated fish, and assessed intestinal abundance by dilution plating. We observed that compared to the wild type *E. coli* strain, the Δ*luxS* strain reached a significantly higher abundance in the intestine (Fig1B).

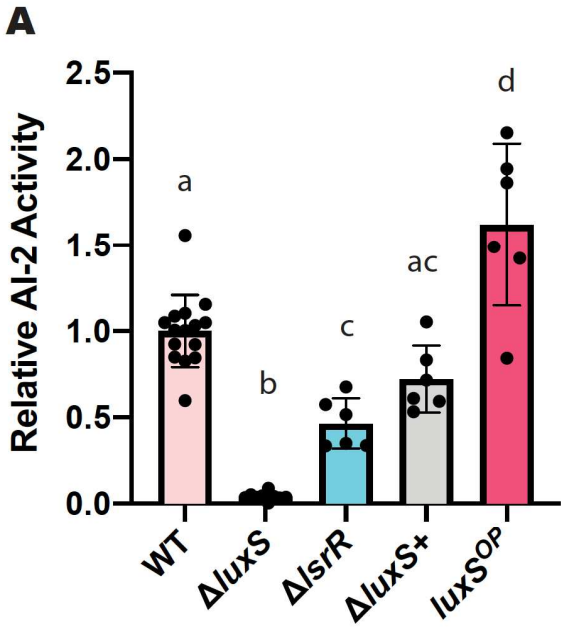

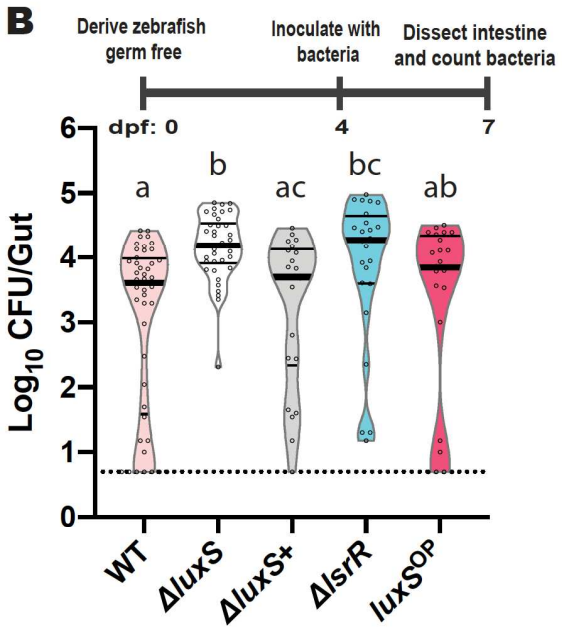

C

Distribution Comparison	K-S Statistic	*p*-value
WT vs *ΔluxS*	**0.4677**	**0.0003**
WT vs *ΔluxS*+	0.1364	0.9479
WT vs *ΔlsrR*	**0.4508**	**0.0036**
WT vs *luxS*^{OP}	0.2386	0.3394

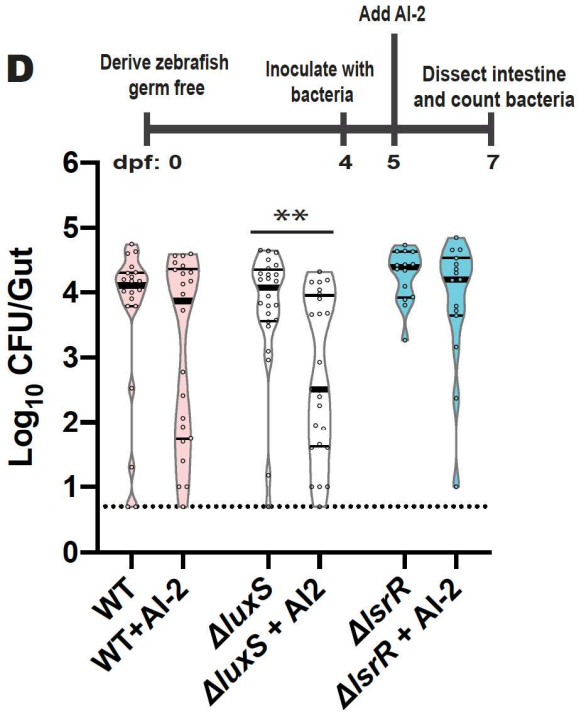

E

Distribution Comparison	K-S Statistic	*p*-value
WT vs WT+AI-2	0.3000	0.3024
***ΔluxS* vs *ΔluxS*+AI-2**	**0.5000**	**0.0050**
ΔlsrR vs *ΔlsrR*+AI-2	0.3286	0.4149

Figure 1. AI-2 signaling reduces intestinal abundance of *E. coli*

(A) AI-2 activity in the cell free supernatant of WT *E. coli,* Δ*luxS,* Δ*lsrR,* Δ*luxS*+ (*luxS* complement), and *luxSOP* (*luxS* overproducer). AI-2 activity was measured through bioluminescence of *V. harveyi* reporter strain TL26. AI-2 reporter activity levels for the mutants were normalized to WT levels. Data shown are the mean with error bars corresponding to SD (n > 6). Letters denote significant differences. $p<0.05$,Tukey's multiple comparison test. (B) Violin plots of intestinal abundance of WT *E. coli,* Δ*luxS,* Δ*lsrR,* Δ*luxS*+ (*luxS* complement), and Δ*luxSOP* (*luxS* overproducer) during mono-association (n>22). Each dot represents one fish intestine, thicker bars in the violin plots denote median and thinner bars denote interquartile ranges. Letters denote significant differences. $p<0.05$, Kruskal-Wallis and Dunn's multiple comparisons test. Experimental timeline is displayed above the graph. (C) Table of Kolmogorov-Smirnov test statistics and corresponding *p*-values. Used to compare relative frequency distributions of mono-association abundance data in Fig1B. (D)Intestinal abundance of WT *E. coli,* Δ*luxS, or* Δ*lsrR* during mono-association after exposure to 100μM AI-2 (n>14). Thicker bars in the violin plots denote median and thinner bars denote interquartile ranges. Significant differences were determined by Mann-Whitney and are denoted by asterisks. ***p=0.0013*. (E) Table of Kolmogorov-Smirnov test statistics and corresponding *p*-values. Used to compare relative frequency distributions of mono-association abundance data in Fig1D.

When we complemented back the *luxS* gene (ΔluxS+) we saw the mean abundance decrease to that of wild type levels (Fig1B). Because *luxS* serves ant metabolic function in the methionine biosynthesis pathway, we wanted to establish whether the difference in intestinal abundance was due solely to the disruption of AI-2 QS or to an altered metabolic state of the cell. In order to do this, we used Δ*lsrR*, a mutant that lacks the transcriptional regulator required for AI-2 QS but in theory maintains a similar metabolic state to wild type. Similar to Δ*luxS* we found that Δ*lsrR* has an increased abundance relative to wild type (Fig1B). This indicates that abolishing AI-2 signaling is the cause of increased bacterial abundance in the zebrafish intestine. This led us to hypothesize that if rather than disrupting AI-2 QS we increased AI-2 signaling we would see a decrease in intestinal abundance. To test this, we measured the intestinal

abundance of *luxS*^{OP} a strain which produces higher amounts of AI-2 (Fig1A). Although we expected a decreased abundance with the AI-2 over-expresser strain, we observed no change when compared to wild type levels (Fig1B). This result may suggest that levels of AI-2 inside the intestine during mono-association with the wild type strain reaches a saturation level for *E. coli* responses that mediate colonization levels.

In addition to exhibiting altered intestinal colonization, the AI-2 signaling mutants also experienced a change in the distribution of abundances across hosts (Fig1B). We note that the fish colonized by wild type *E. coli,* Δ*luxS*+, or *luxS*^{OP} (i.e. strains that are capable of AI-2 QS in the mono-association context) exhibited frequency distributions skewed to lower levels of colonization, with a fraction of fish colonized by just 10 or fewer bacterial cells (Fig1B). However, those fish colonized by Δ*luxS* or Δ*lsrR* (i.e. strains that are unable to experience AI-2 QS in a mono-association) had distributions with a higher percentage of fish being colonized to high levels. As evaluated by the Kolmogorov-Smirnov test, the abundance distributions of both Δ*luxS* and Δ*lsrR* differed significantly from the wild type distribution (Fig1C).

We next tested whether exposure to exogenous sources of AI-2 would lead to changes in intestinal abundance of established *E. coli* communities. To do this we colonized gnotobiotic larval zebrafish with either wild type, Δ*luxS*, or Δ*lsrR*. Following 24 hours after inoculation we added 100μM of purified AI-2 to the water column. After 48hrs of exposure to the exogenous AI-2 we dissected the fish intestines and determined bacterial loads (Fig1D). Addition of AI-2 to the wild type populations did not decrease intestinal abundance, supporting the idea that wild type levels of AI-2 are at a saturation

point. However, the addition of AI-2 resulted in a dramatic increase in the frequency of fish with low colonization levels (Fig 1D). When Δ*luxS* mono-associated fish were exposed to exogenous AI-2, we observed both a significant decrease in the intestinal abundance of Δ*luxS* populations and a shift in the frequency distribution with the group exposed to AI-2 showing an increase in fish colonized to low levels (Fig1D). This change in distributions was confirmed with Kolmogorov-Smirnov test ($p<0.05$) (Fig1E). In contrast, the fish colonized by the Δ*lsrR* that is blind to AI-2 had no observable drop in abundance and the frequency distribution remained largely unchanged after treatment with exogenous AI-2 (Fig1D-E). Collectively, these data support the idea that AI-2 signaling leads to a decrease in intestinal abundance of *E. coli*.

AI-2 signaling reduces the bacterial population in the anterior region of the zebrafish intestine

Based on previous work establishing that aggregated bacterial populations in the intestine are more vulnerable to displacement by gut motility, we hypothesized that the decreased intestinal abundance of *E. coli* in response to AI-2 could be due to increased aggregation. To investigate this possibility, we imaged fluorescent protein expressing *E. coli* in larval zebrafish intestines using both high resolution light sheet microscopy for qualitative assessment and lower resolution stereomicroscopy to evaluate larger numbers of colonized larvae.

Using light sheet fluorescence microscopy we captured images of fish that were colonized with either wild type or Δ*luxS* bacteria. Imaging revealed that *E. coli* was

highly aggregated with almost no planktonic cells (Fig2A-C). In our previous work imaging different bacterial populations in the larval zebrafish, we found that aggregated populations tended to localize to the midgut and occasionally be distally displaced as they were expelled from the gut, whereas populations that consisted of planktonic cells tended to be found in the anterior region of the intestine known as the bulb (41). Consistent with this pattern, *E. coli* aggregates were predominantly localized to the midgut region (Fig2A-C). In some larvae, the Δ*luxS* populations appeared to have a few planktonic cells in the bulb region, but the extremely low number of planktonic cells overall made it difficult to quantify the levels of aggregation between the two populations.

Figure 2. Exposure to exogenous AI-2 displaces Δ*luxS* populations in the zebrafish intestine (next page)

(A) Schematic of a larval zebrafish. Dashed rectangle marks intestinal region imaged by LSFM or with fluorescence dissection microscope. (B) Anatomical regions of the larval zebrafish intestine.(C) Representative maximum intensity projections of WT and Δ*luxS* *E. coli* in mono-association. Images captured by LSFM (n>6). Dashed lines mark intestinal boundaries. The arrowhead points to a multicellular aggregate and the inset is a zoom in of the aggregate designated by the arrowhead. (D) Representative image of Δ*luxS* mono-associations captured with a fluorescence dissecting microscope. Graph depicts the mean intensity curve of Δ*luxS* across length of the intestine (n=15). Shaded region corresponds to SEM and the dotted vertical line corresponds to mean center of mass of the bacterial population. (E) Representative image of Δ*luxS* mono-associations after exposure to 100uM AI-2. Image captured with a fluorescence dissecting microscope. Graph depicts the mean intensity curve of Δ*luxS* across length of the intestine (n=19). Shaded region corresponds to SEM. Dotted vertical line corresponds to mean center of mass of the bacterial population after exposure to exogenous AI-2.

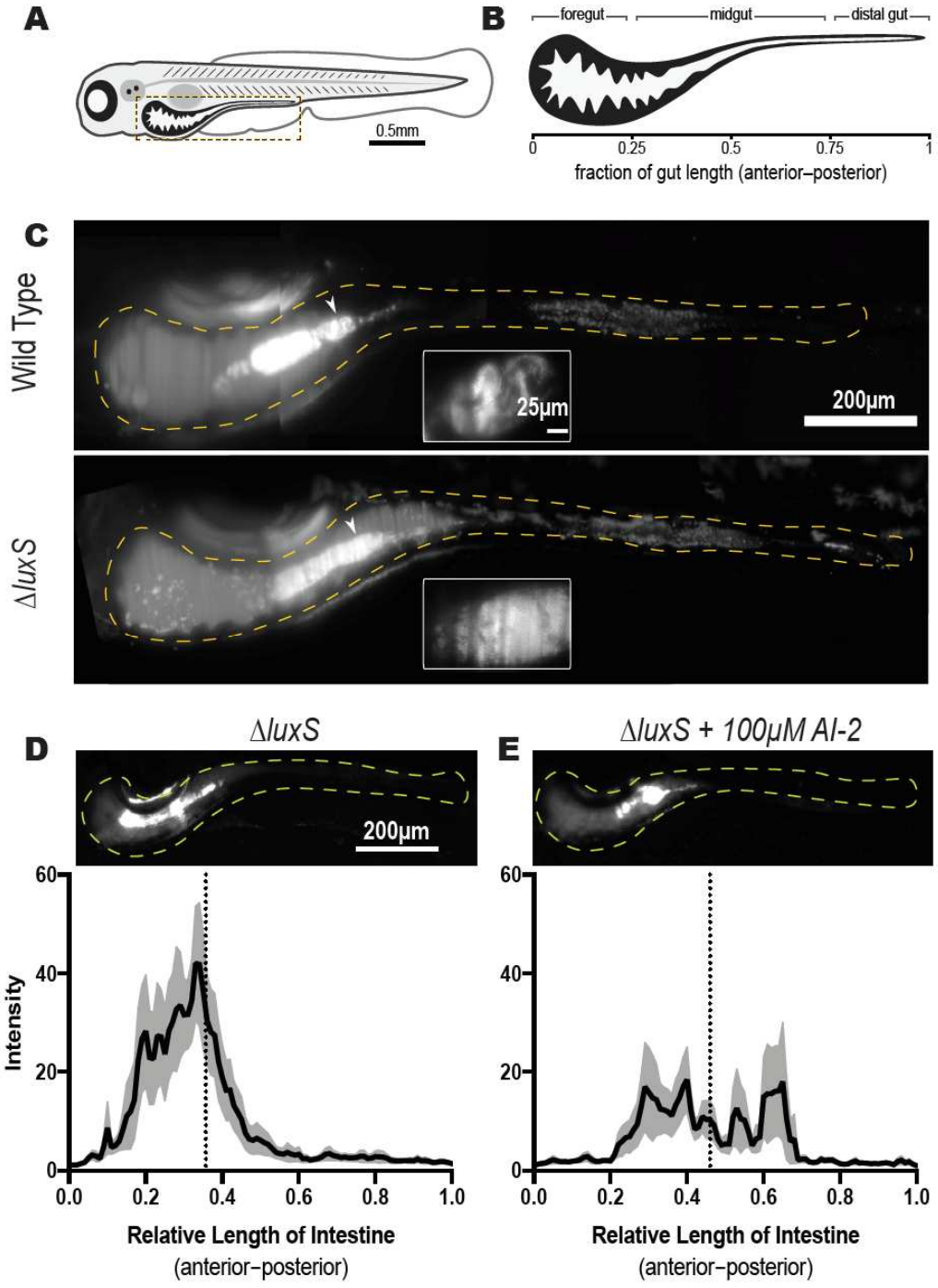

We then turned to stereomicroscopy to determine whether AI-2 treatment altered the large-scale spatial distribution of *E. coli* populations in the intestine. For these

experiments, we used the Δ*luxS* strain which was the most responsive to treatment to exogenous AI-2 in our previous experiments (Fig1D), likely because it has a functional AI-2 reception system without any AI-2 to activate signaling endogenously. We inoculated fish with Δ*luxS E. coli* and 24 hours following the inoculation we added purified AI-2 to the water, exposing the bacterial populations to AI-2 for the following 48 hours prior to imaging on a fluorescent stereomicroscope. We then imaged the entire length of the intestine to evaluate the distribution of the entire intestinal bacterial population. Our analysis of the intensity profiles of Δ*luxS* populations along the intestine revealed that AI-2 treatment resulted in a distal displacement of the bacterial population, with a decrease in the fraction of the population observed in the anterior region and a shift of the center of mass shifted to a more distal region of the midgut (Fig2D-E). These data support the idea that AI-2 signaling increases *E. coli* aggregation, resulting in distal displacement, more frequent expulsion events, and decreases overall intestinal abundance.

In dual-species communities, mutants that alter environmental AI-2 concentrations influence the colonization of their partner strain.

Our results showed that AI-2 signaling differentially altered the intestinal distributions of individual *E. coli* strains with varying AI-2 production and sensing capacities. We next explored how AI-2 would impact mixed communities of these bacterial strains. When we performed di-associations of gnotobiotic larval zebrafish and captured light sheet images of communities composed of the WT and Δ*luxS* strains, we

typically observed aggregated populations organized in multi-strain clusters (Fig3A). We wondered whether co-colonized strains would influence the local AI-2 concentrations experienced by each other. Furthermore, we wondered whether co-aggregating strains would influence each other's susceptibility to distal displacement, resulting in altered patterns of colonization abundances and frequency distributions.

To test if this were the case, we co-inoculated fish with two-strain communities composed of either the wild type or the Δ*luxS* strain paired with either itself, each other, or the Δ*lsrR* or with *luxS*^{OP} strains and then assessed intestinal abundance of both strains in these di-associations (Fig3B). In each combination, both co-colonizing strains were found at similar abundances, with no apparent competitive advantage for any particular strain in the di-associations with the exception of wild type and *luxS*^{OP} di-associations (Fig3C). Notably, the abundance of the wild type strain differed significantly as a function of its partner strain (Fig3B). In the presence of Δ*lsrR*, a strain that depletes environmental AI-2, the wild type strain abundance was significantly greater than when co-colonized with either Δ*luxS,* itself*,* or *luxS*^{OP}(Fig3B), strains that would add no or some additional AI-2 to the environment. The colonization frequency distribution of the wild type strain in the presence of Δ*lsrR* shifted upward resulting in a reduction in the frequency of fish colonized by low levels of bacteria and an increase in fish colonized with high bacterial loads (Fig3B). Comparison of the distributions with a Kolmogorov-Smirnov test, confirms that in the presence Δ*lsrR* and *luxS*^{OP} the abundance distributions of wild type differed significantly from that of wild type partnered co-colonized with itself (Fig3D).

A

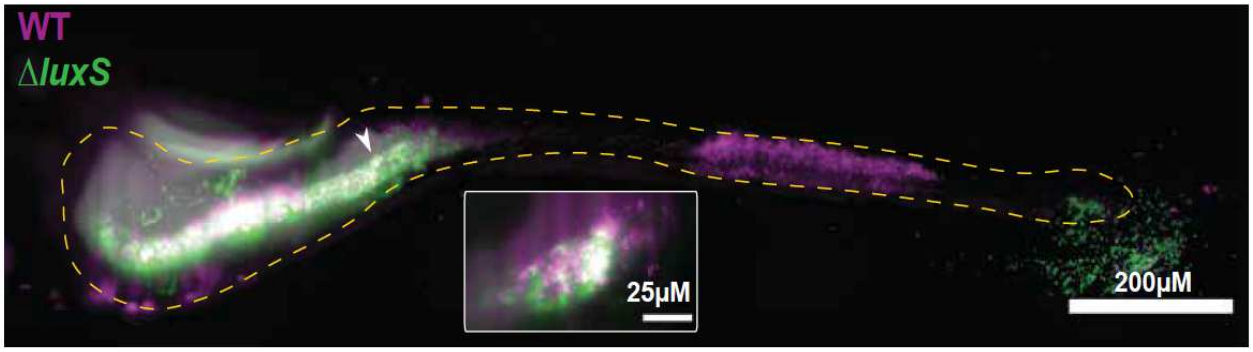

B

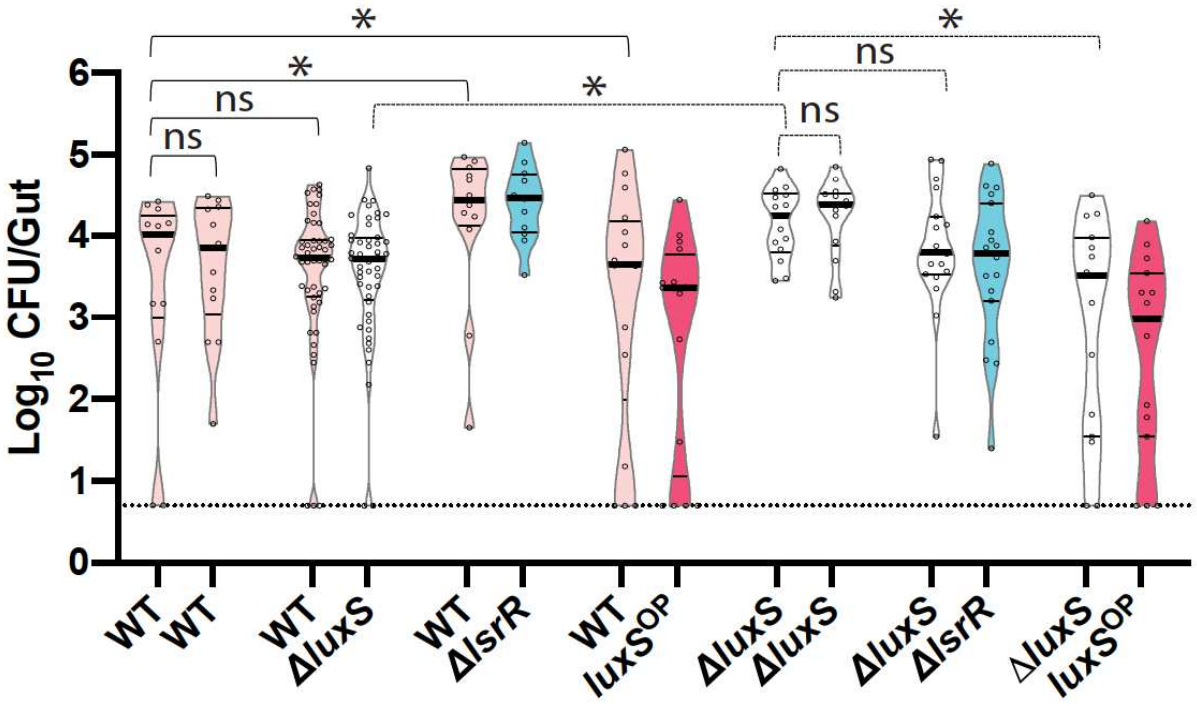

C

Pair	*p*-value (Wilcoxon test)
WT and WT	0.2910
WT and *ΔluxS*	0.2480
WT and *ΔlsrR*	0.5693
WT and *luxS*^{OP}	**0.0344**
ΔluxS and *ΔluxS*	0.7268
ΔluxS and *ΔlsrR*	0.1336
ΔluxS and *luxS*^{OP}	0.0699

D

Distribution Comparison	K-S Statistic	*p*-value
WT_{wt} vs $WT_{\Delta luxS}$	0.3093	0.2817
WT_{wt} vs $WT_{\Delta lsrR}$	0.5192	0.0691
WT_{wt} vs WT_{luxS}^{OP}	0.2404	0.8016
$WT_{\Delta luxS}$ vs $WT_{\Delta lsrR}$	**0.6042**	**0.0018**
$WT_{\Delta luxS}$ vs WT_{luxS}^{OP}	0.2083	0.6749
$WT_{\Delta lsrR}$ vs WT_{luxS}^{OP}	**0.5833**	**0.0188**
$\Delta luxS_{\Delta luxS}$ vs $\Delta luxS_{wt}$	**0.4167**	**0.0464**
$\Delta luxS_{\Delta luxS}$ vs $\Delta luxS_{\Delta lsrR}$	0.3647	0.2340
$\Delta luxS_{\Delta luxS}$ vs $\Delta luxS_{luxS}^{OP}$	0.4667	0.0854
$\Delta luxS_{\Delta luxS}$ vs $\Delta luxS_{wt}$	**0.4167**	**0.0464**
$\Delta luxS_{wt}$ vs $\Delta luxS_{\Delta lsrR}$	0.1897	0.7115
$\Delta luxS_{wt}$ vs $\Delta luxS_{luxS}^{OP}$	0.3167	0.2019
$\Delta luxS_{\Delta lsrR}$ vs $\Delta luxS_{luxS}^{OP}$	0.3614	0.2236
$\Delta lsrR_{\Delta luxS}$ vs $\Delta lsrR_{wt}$	**0.5482**	**0.0240**
$luxS^{OP}{}_{\Delta luxS}$ vs $luxS^{OP}{}_{wt}$	0.2958	0.5070

Figure 3. Co-colonization with AI-2 signaling mutants alters intestinal abundance of *E. coli*

(A) Representative maximum intensity projection of WT *E. coli* and Δ*luxS* di-associations. Images captured by LSFM (n>6). Dashed lines mark intestinal boundaries. Inset is a zoom in of the bacterial cluster designated by the arrowhead. (B) Violin plots of intestinal abundance of WT *E. coli* and AI-2 signaling mutants when co-colonized. $p<0.05$, Kruskal-Wallis and Dunn's multiple comparisons test. The comparisons here are between the WT or Δ*luxS* abundances in each pairing. (C).Table of statistical comparisons of abundances of each strain in the pair using a Wilcoxon test. Bold rows indicate pairings with significantly different abundances. (D) Table of Kolmogorov-Smirnov test statistics and corresponding *p*-values. Used to compare relative frequency distributions of mono-association abundance data in Fig3B. Distributions compared are those of capitalized strain, the subscript indicates what strain it was co-colonized with.

We observed a similar pattern with the Δ*luxS* strain, which differed in mean abundance as a function of its co-colonizing strain (Fig3C). The abundance of Δ*luxS* dropped significantly in the presence of wild type or $luxS^{OP}$ but not when co-colonized with Δ*lsrR* (Fig.3B). It is interesting to note that in all di-associations with Δ*luxS*, the partner strain provided an exogenous source of AI-2 that could reduce its colonization level, as observed with exogenous AI-2 (Fig1D), however it appeared that the amount of AI-2 provided by Δ*lsrR* was insufficient to alter Δ*luxS* abundances. The colonization frequency distributions of Δ*luxS* were also altered dramatically when it was co-colonized with wild type (Fig3D). Collectively our data provide evidence that co-colonizing bacteria, by altering local AI-2 concentrations and by co-aggregating, can influences each other's colonization behaviors.

Exposure to exogenous AI-2 alters intestinal abundance of zebrafish bacterial isolates

The experiments reported so far used a human *E. coli* isolate because of the wealth of knowledge about *E. coli* AI-2 signaling and the genetic tractability of the strain. We next sought to extend these findings to the resident microbiota of the zebrafish. To get a sense of how ubiquitous the production of AI-2 is among native zebrafish gut bacteria, we measured AI-2 activity from overnight cultures of various isolates from our zebrafish gut bacteria culture collection (52). We found that all strains tested, with the exception of a *Pseudomonas,* produced AI-2 (Fig4A).

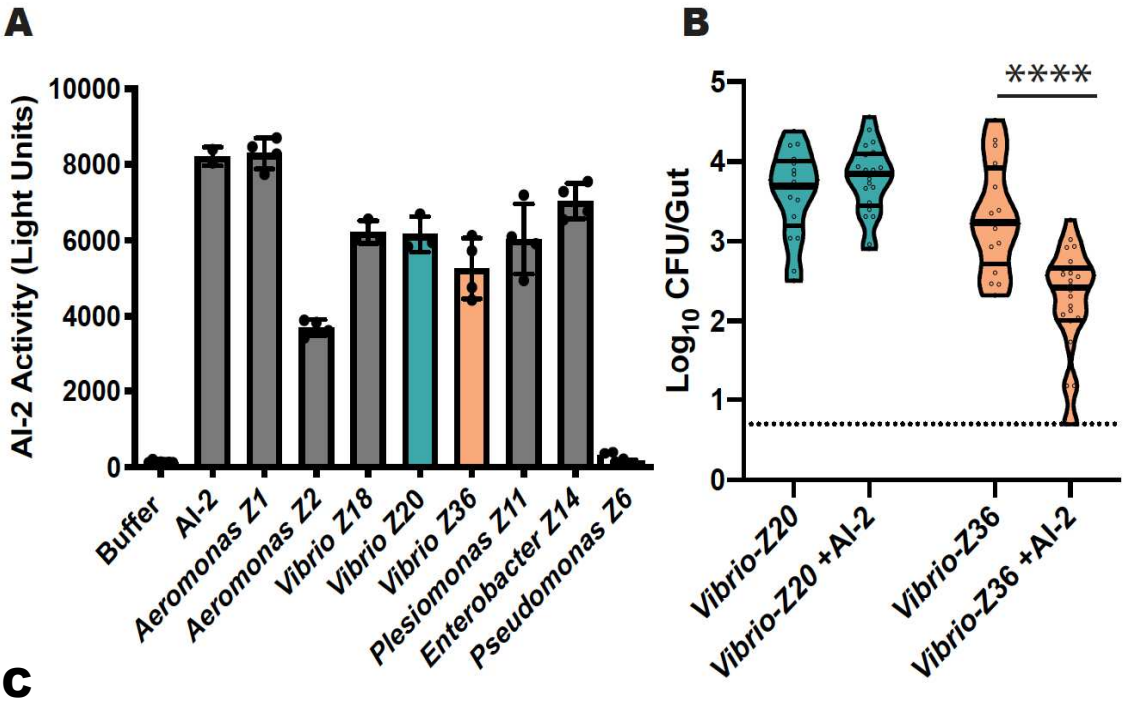

C

Distribution Comparison	K-S Statistic	*p*-value
Vibrio Z20 vs *Vibrio Z20*+AI-2	0.1821	0.9145
***Vibrio Z36* vs *Vibrio Z36*+AI-2**	**0.6250**	**0.0011**

Figure 4. Exposure to AI-2 alters intestinal abundance of zebrafish bacterial isolates. (A) AI-2 activity in the cell-free supernatant of various bacterial isolates native to the zebrafish.Teal and orange bars indicate the AI-2 activity in supernatants of *Vibrio* strains *Z20* and *Z36* respectively. (B) Violin plots of intestinal abundance of *Vibrio-Z20* and *Vibrio-Z36* during mono-association after exposure to 100μM AI-2 (n>16). Each dot represents one fish intestine, thick bars denote median and lighter bars denote interquartile ranges. Asterisks denote significant differences. ****$p<0.0001$, Kruskal-Wallis and Dunn's multiple comparisons test. Dotted line denotes limit of detection for the abundance data. (C) Table of Kolmogorov-Smirnov test statistics and corresponding *p*-values. Used to compare relative frequency distributions of mono-association abundance data in Fig4B.

We then searched for the presence of known AI-2 receptors in the genomes of these isolates and found multiple *Vibrio* strains containing known AI-2 receptors *luxPQ* and other AI-2 signaling associated genes. We chose to focus on strains *Vibrio-Z20* and *Vibrio-Z36* because their genomes resembled that of *Vibrio cholerae,* a species with a well characterized AI-2 signaling pathway (53). Interestingly, these two *Vibrio* strains colonize the zebrafish intestine very differently, with *Z20* being highly planktonic and achieving high colonization levels in the anterior region, whereas *Z36's* population is partially aggregated in the midgut (41). To determine how these strains responded to AI-2, we colonized germ free larval zebrafish with either *Vibrio- Z20* or *Vibrio-Z36* and then exposed the populations to purified AI-2 for 48 hours before assessing intestinal abundance (Fig4B). We found that despite their genomic similarities, these two *Vibrio* strains responded very differently to AI-2. *Vibrio-Z20* displayed no change in intestinal abundance in response to AI-2. In contrast, *Vibrio-Z36* shows a significant drop in abundance after AI-2 exposure (Fig4B). A Kolmogorov-Smirnov test further revealed that treatment with purified AI-2 alters the data distribution of *Vibrio-Z36* (Fig4C).

Discussion

Using the larval zebrafish model we revealed that AI-2 signaling results in decreased intestinal abundance of *E. coli* and shifts bacterial populations from a more anterior region of the intestine to a more distal region (Fig1B,D; Fig2D,E). Additionally, our data demonstrated that in dual-strain communities, strains will influence how their partner strain experiences AI-2 in the intestine resulting in non-autonomous responses to AI-2 that are not predicted by the mono-association data (Fig3B). Bearing in mind that bacterial communities in nature consist of multiple species that have variable capacities to produce and detect environmental AI-2, our work suggests complexities of responses of multispecies communities that can alter local AI-2 environments and change aggregate behaviors through co-aggregation.

Further, we demonstrated that these observations extended to the resident bacteria of zebrafish. We identified several zebrafish isolates that secreted AI-2 (Fig4A) and contained AI-2 receptors in their genomes. We also identified *Vibrio-Z36* as a *Vibrio* species that experiences intestinal collapses after exposure to AI-2. A second zebrafish isolate, *Vibrio-Z20*, that carried the same AI-2 associated genes observed in *Vibrio-Z36* but did not demonstrate any response when exposed to AI-2. This diversity in response to AI-2 from two strains containing the same AI-2 signaling machinery raises the question of why there is an inconsistency between *in vitro* and *in vivo* AI-2 associated phenotypes.

In conclusion, this work established a role for AI-2 signaling in host colonization and bacterial spatial distribution. By characterizing the AI-2 mediated behavior of *E. coli* and extending it to the resident zebrafish isolates we have established a system that will

allow us to pursue remaining questions regarding AI-2 QS in community composition of host associated bacteria. In particular, we now have multiple zebrafish resident bacteria that have been proven to respond to AI-2 in different manners. This allows us to explore the role of AI-2 QS in multi-species communities that have members with varying capacities to produce and sense AI-2. We know from our work with dual strain communities that bacteria that alter environmental AI-2 concentrations in turn affect the response of their neighboring strains to AI-2. While our work was conducted in single species communities, we now propose to extend it to more complex communities which are better representations of communities observed in nature. Lastly it would be interesting to explore why AI-2 mediated *in vitro* behaviors do not translate to an *in vivo* system. Our characterization of *in vivo* AI-2 mediated behaviors in combination with our plate based assays and our capacity to carry out live imaging has expanded our ability to explore the multifaceted role of this ubiquitous bacterial signal.

Methods

Gnotobiotic zebrafish

All zebrafish experiments were performed in accordance with protocols approved by the University of Oregon Institutional Care and Use Committee. Zebrafish husbandry was performed following standard protocols (54). Wild-type (AB x TU strain) zebrafish embryos were derived germ free (GF) as previously described (55). For bacterial associations, bacterial cultures in lysogeny broth (LB) were grown overnight in shaking conditions at 30°C or 37°C. Bacteria were prepared for inoculation by gently pelleting 1 ml of cells and resuspending in sterile embryo media (EM). Bacteria were then added to

the water column of GF flasks at 4 days post fertilization (dpf) at a final concentration of 10^6 CFU/ml. The inoculated flasks were then incubated at 28°C for 72hrs before the zebrafish larvae were sacrificed at 7dpf.

Bacterial strains and culture

Wild- type HS and all *E. coli* HS mutants were grown shaking at 37°C in LB. To generate *E. coli* HS gene deletions we used established protocols (Datsenko and Wanner, 2000; Baba et al., 2006). In brief, we used primers with 40bp homology extensions of the gene of interest to PCR amplify a kanamycin resistance gene flanked by FLP recognition sites. The template used for this amplification was purified from pKD4 plasmid (56, 57). *E. coli HS* carrying pKM208, a plasmid that encodes lambda Red recombinase (58) was then transformed with the PCR product to allow a recombinase mediated replacement of the gene of interest with the kanamycin cassette. Clones were then selected on LB plates with 50µg/ml kanamycin and the pKM208 plasmid, which is temperature sensitive, was cured by growth at 37°C. AI-2 overproducer *luxS*^{OP} and the *luxS* complement Δ*luxS*+ were generated by inserting a copy of *luxS* with its native promoter into the Tn7 insertion site of wild type *E. coli* HS and Δ*luxS,* respectively (Wiles et al., 2018). Both *luxS*^{OP} and Δ*luxS*+ carry a gentamicin resistance gene that was used to select for clones. Fluorescently tagged versions of each strain were generated by Tn7 mediated insertion of a constitutively expressed gene encoding dTomato or sfGFP (59). All fluorescently marked strains carry a gentamicin resistance gene. All zebrafish bacterial isolates, including *Aeromonas* ZOR0001, *Aeromonas* ZOR0002, *Enterobacter* ZOR0014, *Plesiomonas*

ZOR0011, *Pseudomonas* ZWU0006, *Vibrio* ZOR0018, *Vibrio* ZWU0020, and *Vibrio* ZOR0036 (previously describe in PMID: 26339860) were grown shaking at 30°C in LB. All zebrafish bacterial isolates listed were previously described in Stephens *et al* 2016 (52). AI-2 reporter strain *Vibrio harveyi* TL26 was grown shaking at 30°C in Autoinducer Bioassay liquid media (AB).

Measurement of relative AI-2 in liquid culture

An overnight culture of *V. harveyi* TL26 was diluted 1:100 in sterile AB. The diluted culture of *V. harveyi* was then transferred into a white flat bottom 96 well plate (Corning Inc.) with each well holding 190µL of culture. 10µL of cell free supernatant (CFS) harvested from specified bacterial strains were then added into each well holding the 190µL of *V. harveyi* for a total volume of 200µL per well. Bioluminescence and OD_{600} were then monitored over time using a FLU- Ostar Omega microplate reader. *V. harveyi* TL26 only emits light in the presence of exogenous AI-2, therefore only CFS from bacterial strains that produce AI-2 should induce bioluminescence. Readings were taken every 10 minutes until the bacteria were well in stationary phase (approximately 14 hours). The plate reader maintained temperature at 30°C and the plate was shaken between readings. A minimum of three replicate measurements were taken for each CFS sample per experiment and experiments were repeated independently at least twice. In each experiment we included wells with sterile AB that were used as blanks, wells of *V. harveyi* with added buffer that were used as negative controls, and wells of *V. harveyi* with added 10µM purified AI-2 (Omm scientific) that were used as positive controls. We

note that the CFS was harvested on the day of use. To harvest CFS we centrifuged 1ml of an overnight culture for 3 minutes at >11000 x g and then filtered the supernatant through a 0.22-mm sterile tube top filter (Corning Inc.). To determine relative AI-2 activity of all the *E. coli* HS strains, we divided bioluminescence units (LU) by the OD_{600} value for each timepoint. We then normalized the peak LU/ OD_{600} of each strain by dividing the value by the average peak LU/ OD_{600} of wild-type *E. coli.* These resulting values were reported in a bar graph (Fig.1A) as "Relative AI-2 activity." Tukey's multiple comparison test was used to compare the mean relative AI-2 activity of all groups. Statistical analysis and data plotting were done using GraphPad Prism 7.

Quantification of bacterial populations

At 7dpf larvae were euthanized with tricaine and mounted in 3% methylcellulose. Dissection of larval intestines was done as previously described (60). Dissected intestines were placed in an Eppendorf tube with 500µl of sterile 0.7% saline and 100µl 0.5 mm zirconium oxide beads. Intestines were then homogenized using a bullet blender tissue homogenizer for 1.5 minutes on power 4. Lysates were then serially plated on LB (for samples containing *E. coli*) or TSA (for samples containing *Vibrio*). After overnight incubation at 30°C, colonies to determine CFUs/gut. Samples with no detectable colonies on the plate with the lowest dilution were set to the limit of detection (5 bacteria per gut). For each experiment, a sample of the water column was also serially plated to enumerate the CFUs in each flask. The water samples used for plating were collected at 4dpf after inoculation of the water column and at 7dpf after dissection of larvae. Each experiment

contained a minimum of 8 fish per group and was repeated at least twice. Statistical differences between multiple groups (Fig.1B, Fig.3B) were determined by Kruskal-Wallis and Dunn's multiple comparisons tests. Statistical differences between two groups were determined by the Mann-Whitney test (Fig.1C). Statistical differences between two paired groups of data were determined by the Wilcoxon test (Fig.3B). To compare the frequency distributionof bacterial abundances across groups, the Kolmogorov-Smirnov test was performed. GraphPad Prism 7 was used to perform all statistical analysis and plot data.

Addition of exogenous AI-2 to established bacterial communities

GF zebrafish flasks were inoculated with the specified bacteria at 4dpf. 24 hours were allowed for the bacteria to colonize the larvae and at 5dpf purified AI-2 (Omm Scientific) was added to the water column for a final concentration of 100μM. The purified AI-2 used for these experiments arrived dissolved in 0.5mM $NaHSO_4$ with a pH of 2-3 (depending on the batch), therefore as a control we added the same volume of 0.5mM $NaHSO_4$ to a second flask that was inoculated with the same bacterial strain. After addition of either the AI-2 or the $NaHSO_4$, we measured the pH of the water column of each flask to ascertain that there were no dramatic shifts in pH following the addition of the acidic compounds. The pH of the water columns always fell between pH 7.5-8 and was not notable difference between the control and treatment flasks. After 48 hours of exposure to the AI-2 or $NaHSO_4$, the zebrafish at 7dpf were either imaged or processed for quantification of bacterial populations by dilution plating. Each experiment contained a minimum of 7 fish per group and each experiment was performed at least twice.

Live imaging of larval zebrafish

Fluorescent light sheet microscope: For high resolution, qualitative analysis of bacterial aggregation in the larval intestine, live larval zebrafish that had been colonized with fluorescent bacteria were imaged at 7dpf using a custom built light sheet fluorescence microscope previously described (51). Larvae were anesthetized with tricaine and mounted into small glass capillaries containing 0.5% low melt agarose. The zebrafish larvae were then suspended in a custom imaging chamber containing sterile EM and tricaine until the agarose set. The agarose embedded larvae were then extruded from the end of the capillary and oriented so that the digestive tract was facing the imaging objective. The entire length of the intestine was then imaged in 4 subregions. Six fish were imaged for each group.

Fluorescent stereomicroscope: For higher throughput, lower resolution imaging, live larval zebrafish that had been colonized with fluorescent bacteria were imaged at 7dpf using a Leica MZ10 Fluorescence stereomicroscope with a 1.0X objective. Larvae were anesthetized with tricaine and mounted onto a glass slide coated with 3% methylcellulose. Fish were oriented so that they lay on their left side with their gut facing the imaging objective. An image of the entire intestine was then captured. Quantitative image analysis was performed in Fiji. Using a free hand line tool set at 30 pixels, a line was drawn from the anterior to the posterior end of the digestive tract, following the natural curve of the intestine and encompassing all fluorescently labelled colonizing bacterial clusters. To remove any background fluorescence produced by the tissues surrounding the intestine, we used the background subtraction tool in Fiji with a rolling ball radius set at 15 pixels. We then used the plot profile tool to display the fluorescence

intensity profile along the line spanning the length of the intestine. This tool provides an intensity value (y-value) at each point along the length of the line (x-value). To account for differences in the size of fish, all x-values were divided by the total length of line to report the relative length of the intestine of each fish. GraphPad Prism 7 was used to plot the average intensity profiles across the relative length of the intestine for each group of fish. The center of mass of the bacterial populations were determined for each fish using the following equation:

Center of mass = Sum(position × intensity) / Sum(intensity).

A minimum of 13 fish were imaged for each treatment group.

CHAPTER III

BIOINFORMATIC COMPARISON OF AI-2 QS GENES IN *VIBRIO* STRAINS

Introduction

In Fig.4 of chapter II we determined that AI-2 QS phenotypes observed with *E. coli* extend to the resident microbiota of the zebrafish. Not only was AI-2 production wide-spread among zebrafish commensal isolates but several *Vibrio* isolates contained AI-2 QS gene networks. We chose to focus on strains *Vibrio-Z20* and *Vibrio-Z36* due to the fact that their genomes resembled that of *Vibrio cholerae,* a species with a well characterized AI-2 signaling pathway. We determined that larval zebrafish colonized with *Vibrio-Z36* and then exposed to exogenous AI-2 experienced drops in intestinal abundance of *Vibrio*. This did not hold true for *Vibrio- Z20* where no change in intestinal abundance was observed (Fig 4B). Of interest, we note that in liquid culture *Vibrio- Z20* grows as motile, planktonic cells while *Vibrio-Z36* forms large clusters that settle out of solution. A similar observation is made in the larval intestine where *Vibrio-Z20* resides in the bulb as a predominantly planktonic motile population while *Vibrio-Z36* has a subset of its population that is clustered in non-motile aggregates and localizes in the midgut (24). We wondered whether similar to *E. coli,* AI-2 was mediating aggregation or biofilm formation in *Vibrio-Z36* resulting in displacement of cells in the intestine. If this were the case, it raises the question of why two *Vibrio* species that contain the same AI-2 QS gene

networks respond so differently to AI-2. To answer these questions, we tested the hypothesis that AI-2 mediates aggregation in *Vibrio.* Further we compared the genetic sequences of the AI-2 associated genes in the genomes of these two strains in an attempt to identify dissimilarities that might result in the differing AI-2 responses between the *Vibrio-Z20* and *Vibrio-Z36.*

Results and Discussion

AI-2 treatment induces *Vibrio-Z20* aggregation in a chemotaxis dependent manner

We carried out a crystal violet biofilm assays to determine if either *Vibrio-Z20 or Z36* displayed an aggregation phenotype in response to exogenous AI-2 treatment. Unexpectedly, we observed that *Vibrio-Z20* but not *Vibrio-Z36* showed increased biofilm formation when treated with purified AI-2 (Fig 5A-B). Interestingly, when this biofilm assay was performed with a chemotaxis mutant of *Z20* (Δ*cheA2/3*) the AI-2-responsive biofilm formation was no longer observed, suggesting that AI-2 mediated biofilm formation in *Z20* is dependent on chemotaxis (Fig5A).

Figure 5. *Vibrio- Z20* but not *Vibrio- Z36* exhibits AI-2 mediated aggregation *in vitro* (next page)

(A) Biofilm formation assay of *Vibrio- Z20* (teal) and Δ*cheA2/3 Z20* (black) after treatment with purified AI-2. Letters denote significant differences between wild type groups, $p<0.5$. There were no significant differences between Δ*cheA2/3 Z20.* One way ANOVA was performed for comparison of treatments. Each dot represents one biofilm. (B) Biofilm formation assay of *Vibrio- Z36* (orange) after treatment with purified AI-2. One way ANOVA was performed for comparison of treatments, but no significant difference was detected. (C) Capillary assays of *Vibrio- Z20* (teal) and Δ*cheA2/3 Z20* (black) to test chemotaxis response to AI-2. Asterisks denote significant differences as identified by unpaired t-tests, $p< 0.0001$. (D) Capillary assays of *Vibrio- Z36* (orange) to

test chemotaxis response to AI-2. Unpaired t-tests were performed but no significant differences were identified. Each dot represents one sample.

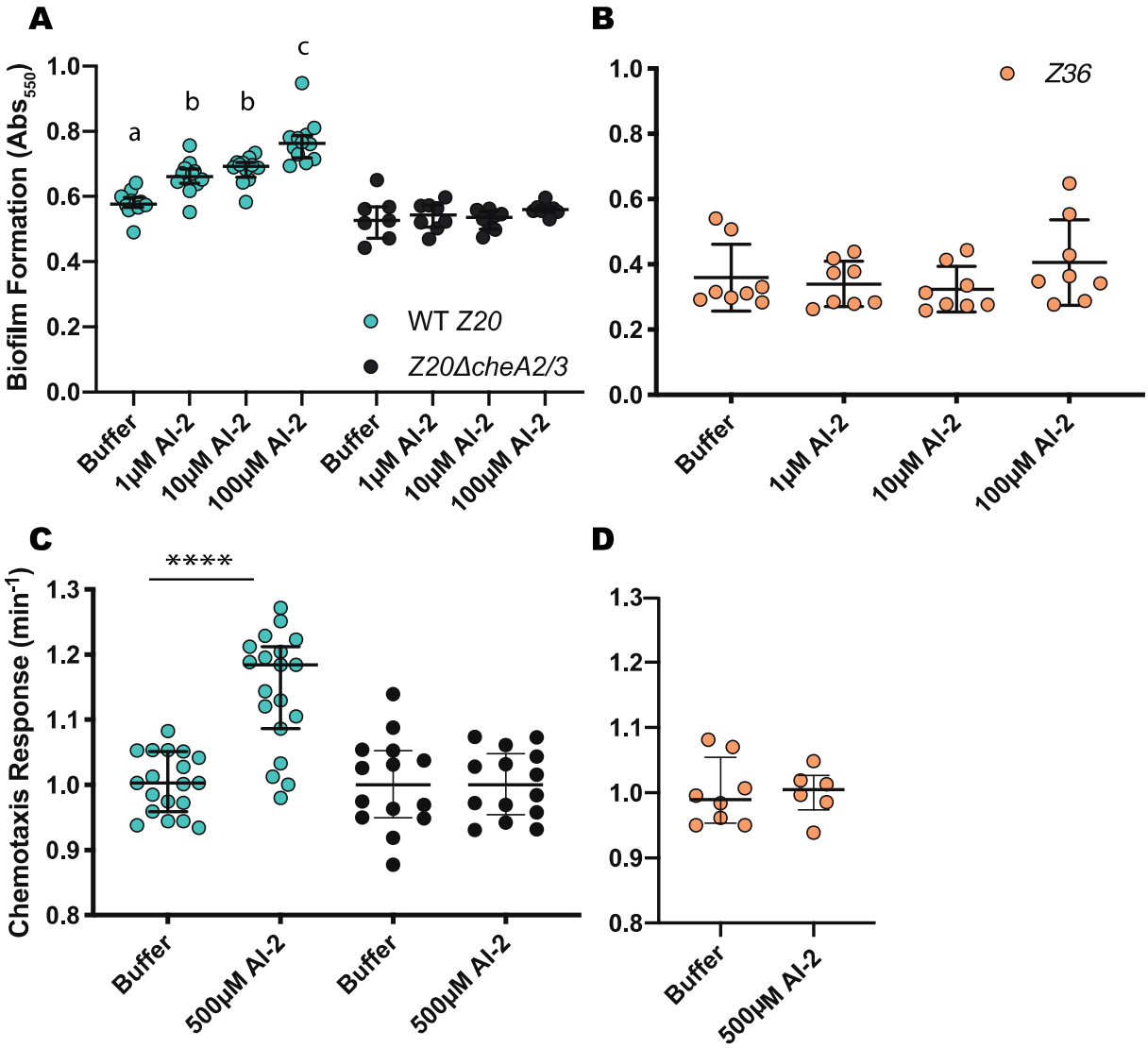

Our finding that the Δ*cheA2/3 Z20* mutant failed to form biofilms in response to AI-2 inspired us to perform a chemotaxis assay to determine if similar to *E. coli* and *H. pylori*, *Vibrio* perceived AI-2 as a chemoeffector. A capillary assay revealed that AI-2 was a chemoattractant for *Vibrio-Z20* but not *Vibrio-Z36* (Fig5C-D). These finding were

notable because they constitute the first report of any *Vibrio* species sensing an autoinducer as a chemotactic cue and suggested that similar to *E. coli* and *H. pylori*, AI-2 has the potential to alter spatial structuring of *Vibrio-Z20* communities.

Variation in the LuxP AI-2 binding pocket

Taking into consideration the data presented in Fig4B where it is *Z36* not *Z20* that shows a change in abundance in the zebrafish gut when exposed to AI-2, we expected to see *Z36* not *Z20* show a response of aggregation in the *in vitro* biofilm assays. The unexpected results made us wonder why two genetically similar strains that reside in the same environment and carry the same AI-2 quorums sensing networks show such variation in AI-2 responses. To further explore this we carried out amino acid sequence comparisons to search for regions of the known proteins involved in AI-2 response. AI-2 signaling in *Vibrio spp* have been extensively studied (25, 53, 61–63) but briefly involves the detection of AI-2 via binding of periplasmic protein LuxP which initiates a signaling cascade that travels through membrane bound protein LuxQ, and cytoplasmic proteins LuxO and LuxU ultimately resulting in changes in gene expression (Fig6A). Amino acid sequence alignments of LuxP, LuxQ, LuxO, and LuxU revealed a high conservation between these *Z36* and *Z20* (Fig6B). We chose to look more closely at the differences in LuxP as it was the least conserved. The residues important for establishing hydrogen bonding in the LuxP - AI-2 binding pocket had been previously identified in a LuxP structure of *V. harveyi* (Fig6C). We noted that in particular residue 266 which is normally an arginine, is actually a glycine in *Vibrio-Z20*. While we do not have the structure of *Vibrio-Z20* we know from

the *V. harveyi* that this residue plays an important function in establishing polar contacts with AI-2. It is therefore possible that in *Z20* the lack of arginine makes *Z20* LuxP less capable of binding AI-2 and therefore less sensitive to AI-2 exposure in the intestine. However this difference does not explain why we observe AI-2 responses *in vitro* for this strain but not for *Z36.* We also looked more closely at the amino acid changes in each gene but were not able to identify important residue changes. It is possible that some of the observed changes are of importance but we lack annotations of important residues for each protein involved in AI-2 sensing.

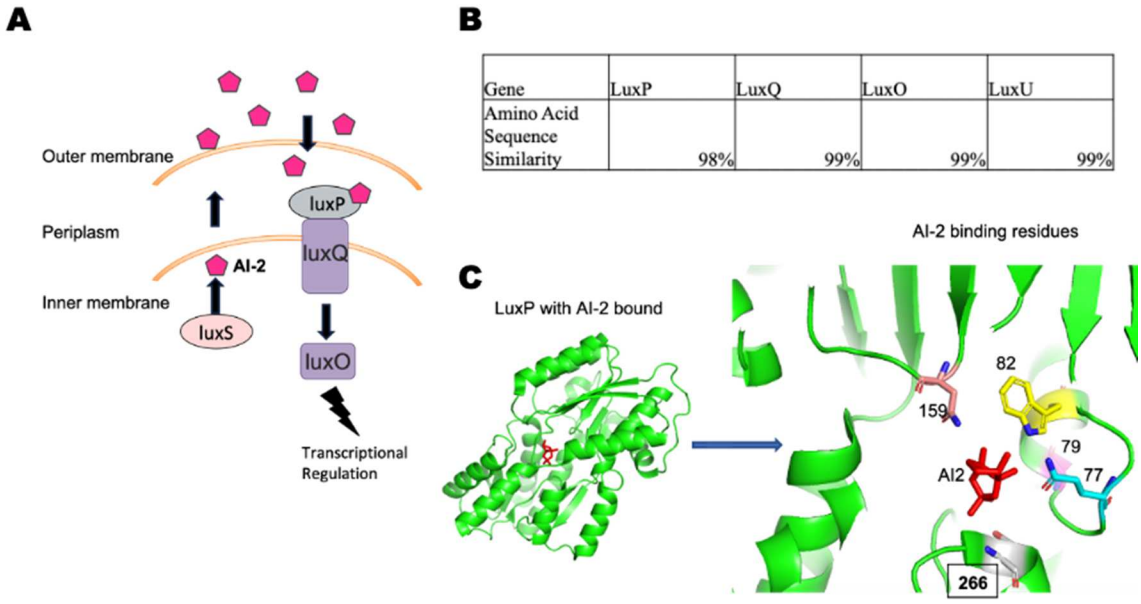

Figure 6: AI-2 QS genes have high sequence conservation of amino acids
(A) Simplified AI-2 sensing pathway in *Vibrio* characterized by production of AI-2 via LuxS and detection of AI-2 via LuxP binding and a phosphorelay with LuxO. (B) Table showing amino acid sequence conservation in AI-2 associated genes between *Z20* and *Z36.* (C) Structure of LuxP with bound AI-2. Arrow points to a zoom in of the AI-2 binding pockets with important binding residues annotated. The boxed residue 266 arginine in the *Vibrio harveyi* structure is predicted to be conserved in *Z36* but changed to a glycine in *Z20*.

While it is clear that there is high conservation of AI-2 QS associated genes between these two strains and while one notable difference was observed in the LuxP binding site, we still lack an understanding for why these two isolates experience AI-2 so differently in the intestine and in biofilms. In the future it would be interesting to further explore what results in these discrepancies between strains and between *in vivo* and *in vitro* contexts.

Methods

Bacterial Cultures

Vibrio ZWU0020 and *Vibrio* ZOR0036 were grown overnight shaking at 30°C in Tryptone Broth (TB).

Crystal Violet Biofilm Assays

Overnight cultures of *Vibrio* ZWU0020 or *Vibrio* ZOR0036 were diluted 1:1000 in sterile TB. 100µL of diluted culture were then added to the wells of a polystyrene 96 well plate. Purified AI-2 was then added to the wells with cells for a final concentration of either 0µM AI-2, 1µM AI-2, 10µM AI-2, or 100µM AI-2. The plate was then incubated at 30°C for 24 hours. After incubation the plate was inverted and the cells were gently shaken out of the wells and discarded. The wells were then gently washed with ddH_2O three times to dislodge any non-adherent cells. The wells were then filled with 150µL 0.3% crystal violet and the plate was allowed to sit at room temperature for 10 minutes. The crystal violet was then discarded and the plate was washed with ddH_2O three times to remove any excess crystal violet. The wells were then filled with DMSO to de-stain the biofilms of crystal violet. The plate was then incubated at room temperature for 15 minutes. A 100

μL sample was then taken from each well and transferred to a clean microtiter plate. The absorbance at 550 was then measured for each well.

Capillary Assays

Overnight cultures of *Vibrio* ZWU0020 or *Vibrio* ZOR0036 were diluted 1:1000 in 20mL of sterile TB and placed at 30°C shaking until the culture reached OD_{600} of 0.4-0.6. 1mL of cells were then gently pelleted and resuspended in 5 mL of sterile 1xPBS. The cells in PBS were then kept at room temperature and allowed to recover for 15-25 minutes. The motility of the cells was monitored to assure that cells were swimming. Once cells were observed to be motile, 100μL of cells were added to the wells of a microtiter plate. 5μL pipette tips were then filled with the chemoeffectors to be tested. The pipette tips were then settled into the cell suspensions and allowed to remain there for 30 minutes to allow cells to swim into the pipette tips. After 30 minutes the pipette tips were removed and the contents were expelled into a microtiter plate with sterile LB. The plate was then placed in FLU- Ostar Omega microplate reader and OD_{600} was monitored over time for ~14 hours. Readings were taken every 10 minutes. Experiment was repeated 2-3 times and each experiment had a minimum of 8 replicates. For each sample we then determined the time it took for OD_{600} to reach 0.5 and was normalized to the time it took the control to reach OD_{600} 0.5 .The inverse of this value was then reported as the "chemotaxis response." Those samples that reached this OD faster (had a chemotaxis response larger than 1) started off with more cells suggesting that the chemoeffector in the pipette tip was a chemoattractant. For those samples that took longer to reach this OD (had a chemotaxis response smaller than 1) started off with less cells suggesting that the chemoeffector in the pipette tip was a

chemorepellent. This assay was modified from the high throughput capillary assay described by Bainer *et al* 2003 (64).

Bioinformatic Analysis

Sequences of *Vibrio* ZWU0020 and *Vibrio* ZOR0036 were taken from Joint Genome Institute. IMG Genome ID for *Vibrio* ZWU0020 is 2703719078 and for *Vibrio* ZOR0036 is 2703719079. IMG Genome ID for *Vibrio cholerae* C6706 is 2663763252. Sequence alignments were carried out using ApE genome editor. Pymol was used to look at PDB structures of *V. harveyi.*

CHAPTER VI

CONCLUDING REMARKS

Characterization of the zebrafish gut ecosystem has revealed that the inherent cohesiveness of the bacterial communities, in combination with host intestinal movements, impacts the composition and spatial distribution of the microbiota (41–44). Therefore, factors that govern bacterial cohesion, such as AI-2, are likely to shape the membership and biogeography of bacterial communities within the intestine. Using the larval zebrafish model, we have described the role of widespread QS signal, AI-2, in colonization and spatial distribution of bacteria in a vertebrate host. We revealed that AI-2 signaling results in decreased intestinal abundance of *E. coli* and leads to the displacement of bacterial populations from a more anterior region of the intestine to a more posterior region. Our data further demonstrated that in dual-strain populations, strains will influence how the other experiences AI-2 in the intestine, resulting in non-cell autonomous responses to AI-2. Considering that microbial communities in nature are complex, consisting of multiple species that have varying capacities to produce and detect environmental AI-2, our work suggests possible complexities of responses of multispecies communities that can alter local AI-2 environments and change community behaviors through co-aggregation.

Our observations also extend to the resident bacteria of zebrafish. We found that a majority of strains secrete AI-2 and several contain AI-2 receptors in their genomes. In particular we identified *Vibrio-Z36* as a *Vibrio* species that experiences intestinal

collapses after exposure to AI-2. We identified a second zebrafish isolate, *Vibrio-Z20*, that carried the same AI-2 associated genes observed in *Vibrio-Z36* but did not exhibit any response when exposed to AI-2 *in vivo*. Interestingly, we observed that *in vitro Vibrio-Z20* aggregates and forms biofilms in response to AI-2 exposure. This behavior was chemotaxis dependent and AI-2 was further proven to serve as a chemoattraction signal for *Vibrio-Z20*. Surprisingly, we did not observe any response to AI-2 from *Vibrio-Z36* using *in vitro* methods. This diversity in response to AI-2 from two strains containing the same AI-2 sensing machinery, indicates that there are unaccounted complexities in host system. In particular this poses the question of why there is a discrepancy between *in vitro* and *in vivo* AI-2 associated phenotypes.

Currently AI-2 is the only autoinducer known to serve as both a QS signal and a chemotaxis signal. Although not a chemoeffector for all bacteria, AI-2 has been shown to be a repellant for the gastric pathogen *H. pylori* and an attractant for both pathogenic and commensal *E. coli* (13, 27, 28, 40, 46, 47, 49). My work adds to this list by demonstrating that AI-2 is a chemoattractant for *Vibrio-Z20*. These findings suggests that AI-2 not only has the potential to alter distribution of bacterial populations through the slower acting mechanism of gene regulation but also, by serving as a chemotactic cue, AI-2 has the potential to recruit or disperse bacteria to bacterial aggregates on fast time scales (11, 17, 27, 47). In work I contributed to, agent based modeling demonstrated how AI-2 chemotaxis could alter the architecture of bacterial biofilms (40).

While quorum sensing has traditionally been considered as a bacterial specific form of communication, there are a growing number of reports indicating that the host

can also join in on the conversation. In fact both mammalian cells and plant cells have been reported to have QS signal receptors (5, 65, 66). For example, human upper airway epithelial cells detect QS signals of both Gram negative and Gram positive microbes. When the upper airway epithelium senses the presence of autoinducers, they produce the antibacterial molecule, Nitric Oxide (NO) (67, 68).It was also reported that mammalian epithelial cells exposed to AI-2 produced inflammatory cytokine interleukin-8 (69). These two mechanisms provide a way for the host to clear particular bacterial members via detection of autoinducers. Although similar host responses to AI-2 have not yet been described in the zebrafish intestine, it would not be surprising for processes described in mammals and plants to be found in fish.

In addition to detecting bacterial autoinducers, mammalian epithelial cells were also shown to secrete AI-2 mimics in response to the presence of bacteria (50). This AI-2 mimic was detected by the traditional AI-2 receptors, LsrB (*E. coli*) and LuxP (*V. harveyi*) both of which are receptors found in the strains we worked with (50). Given the ubiquity of AI-2 QS among bacterial residents of the zebrafish intestine, it may be advantageous for this tissue to produce an AI-2 mimic to influence the behavior of its microbiota members and ultimately promote or exclude particular bacterial strains by inducing aggregation or dispersal from aggregates.

In conclusion, my work establishes a role for AI-2 signaling in vertebrate intestinal colonization and bacterial spatial distribution. By characterizing the AI-2 mediated behavior of *E. coli* and extending it to the resident zebrafish isolates I have laid the foundation to pursue further questions regarding AI-2 QS in community composition

of host associated bacteria. In particular, I have demonstrated the AI-2 production and responses of multiple zebrafish resident species. This knowledge will allow us to explore the role of AI-2 QS in multi-species communities that have members with varying capacities to produce and sense AI-2. We know from my work with dual strain communities that bacteria that alter environmental AI-2 concentrations in turn affect the AI-2 responses of their co-habiting strains. The next stage of this work will be to extend characterizations to more complex communities which are better representations of communities observed in nature. Our gnotobiotic zebrafish system is amenable to live imaging studies that can be used to separate the impacts on bacterial population spatial distributions of AI-2 QS versus AI-2 chemotaxis, which operate on different time scales. Lastly it would be interesting to explore why AI-2 mediated *in vitro* behaviors do not translate to an *in vivo* system. Our characterization of *in vivo* AI-2 mediated behaviors in conjunction with our plate-based assays and our capacity to carry out live imaging has expanded our ability to explore the multifaceted role of this widespread bacterial signal.

REFERENCES CITED

1. Nealson KH, Platt T, Hastings JW. 1970. Cellular Control of the Synthesis and Activity of the Bacterial Luminescent System1. J Bacteriol 104:313–322.

2. Fuqua WC, Winans SC, Greenberg EP. 1994. Quorum sensing in bacteria: the LuxR-LuxI family of cell density-responsive transcriptional regulators. J Bacteriol 176:269–275.

3. Whiteley M, Diggle SP, Greenberg EP. 2017. Progress in and promise of bacterial quorum sensing research. Nature 551:313–320.

4. Parsek MR, Greenberg EP. 2000. Acyl-homoserine lactone quorum sensing in Gram-negative bacteria: A signaling mechanism involved in associations with higher organisms. Proc Natl Acad Sci 97:8789–8793.

5. Papenfort K, Bassler BL. 2016. Quorum sensing signal–response systems in Gram-negative bacteria. Nat Rev Microbiol 14:576–588.

6. Xavier KB, Bassler BL. 2003. LuxS quorum sensing: more than just a numbers game. Curr Opin Microbiol 6:191–197.

7. Bassler BL. 1999. How bacteria talk to each other: regulation of gene expression by quorum sensing. Curr Opin Microbiol 2:582–587.

8. Miller MB, Bassler BL. 2001. Quorum Sensing in Bacteria. Annu Rev Microbiol 55:165–199.

9. Bhatt VS. 2018. Quorum Sensing Mechanisms in Gram Positive Bacteria, p. 297–311. *In* Pallaval Veera Bramhachari (ed.), Implication of Quorum Sensing System in Biofilm Formation and Virulence. Springer, Singapore.

10. Rutherford ST, Bassler BL. 2012. Bacterial Quorum Sensing: Its Role in Virulence and Possibilities for Its Control. Cold Spring Harb Perspect Med 2.

11. Niu C, Robbins CM, Pittman KJ, Osborn joDi L, Stubblefield BA, Simmons RB, Gilbert ES. 2013. LuxS influences Escherichia coli biofilm formation through autoinducer-2-dependent and autoinducer-2-independent modalities. FEMS Microbiol Ecol 83:778–791.

12. Vendeville A, Winzer K, Heurlier K, Tang CM, Hardie KR. 2005. Making “sense” of metabolism: autoinducer-2, LuxS and pathogenic bacteria. Nat Rev Microbiol 3:383–396.

13. Bansal T, Jesudhasan P, Pillai S, Wood TK, Jayaraman A. 2008. Temporal regulation of enterohemorrhagic Escherichia coli virulence mediated by autoinducer-2. Appl Microbiol Biotechnol 78:811–819.

14. Bearson BL, Bearson SMD. 2008. The role of the QseC quorum-sensing sensor kinase in colonization and norepinephrine-enhanced motility of Salmonella enterica serovar Typhimurium. Microb Pathog 44:271–278.

15. Lupp C, Ruby EG. 2005. Vibrio fischeri Uses Two Quorum-Sensing Systems for the Regulation of Early and Late Colonization Factors. J Bacteriol 187:3620–3629.

16. Wei H-L, Zhang L-Q. 2006. Quorum-sensing system influences root colonization and biological control ability in Pseudomonas fluorescens 2P24. Antonie Van Leeuwenhoek 89:267–280.

17. Rader BA, Wreden C, Hicks KG, Sweeney EG, Ottemann KM, Guillemin K. 2011. Helicobacter pylori perceives the quorum-sensing molecule AI-2 as a chemorepellent via the chemoreceptor TlpB. Microbiology 157:2445–2455.

18. Barrios AFG, Zuo R, Hashimoto Y, Yang L, Bentley WE, Wood TK. 2006. Autoinducer 2 Controls Biofilm Formation in Escherichia coli through a Novel Motility Quorum-Sensing Regulator (MqsR, B3022). J Bacteriol 188:305–316.

19. Auger S, Krin E, Aymerich S, Gohar M. 2006. Autoinducer 2 affects biofilm formation by Bacillus cereus. Appl Environ Microbiol 72:937–941.

20. Abisado RG, Benomar S, Klaus JR, Dandekar AA, Chandler JR. 2018. Bacterial Quorum Sensing and Microbial Community Interactions. mBio 9:e02331-17.

21. Greenberg EP. 2000. Acyl-Homoserine Lactone Quorum Sensing in Bacteria. J Microbiol 38:117–121.

22. Parsek MR, Greenberg EP. 2000. Acyl-homoserine lactone quorum sensing in gram-negative bacteria: a signaling mechanism involved in associations with higher organisms. Proc Natl Acad Sci U S A 97:8789–8793.

23. Pereira CS, Thompson JA, Xavier KB. 2013. AI-2-mediated signalling in bacteria. FEMS Microbiol Rev 37:156–181.

24. Papenfort K, Bassler B. 2016. Quorum-Sensing Signal-Response Systems in Gram-Negative Bacteria. Nat Rev Microbiol 14:576–588.

25. AI-2-mediated signalling in bacteria | FEMS Microbiology Reviews | Oxford Academic.

26. Xavier KB, Bassler BL. 2003. LuxS quorum sensing: more than just a numbers game. Curr Opin Microbiol 6:191–197.

27. Anderson JK, Huang JY, Wreden C, Sweeney EG, Goers J, Remington SJ, Guillemin K. 2015. Chemorepulsion from the Quorum Signal Autoinducer-2 Promotes Helicobacter pylori Biofilm Dispersal. mBio 6:e00379.

28. Hegde M, Englert DL, Schrock S, Cohn WB, Vogt C, Wood TK, Manson MD, Jayaraman A. 2011. Chemotaxis to the Quorum-Sensing Signal AI-2 Requires the Tsr Chemoreceptor and the Periplasmic LsrB AI-2-Binding Protein. J Bacteriol 193:768–773.

29. Mok KC, Wingreen NS, Bassler BL. 2003. Vibrio harveyi quorum sensing: a coincidence detector for two autoinducers controls gene expression. EMBO J 22:870–881.

30. Cuadra GA, Frantellizzi AJ, Gaesser KM, Tammariello SP, Ahmed A. 2016. Autoinducer-2 detection among commensal oral streptococci is dependent on pH and boric acid. J Microbiol 54:492–502.

31. Cuadra-Saenz G, Rao DL, Underwood AJ, Belapure SA, Campagna SR, Sun Z, Tammariello S, Rickard AH. 2012. Autoinducer-2 influences interactions amongst pioneer colonizing streptococci in oral biofilms. Microbiology 158:1783–1795.

32. Wang Z, Xiang Q, Yang T, Li L, Yang J, Li H, He Y, Zhang Y, Lu Q, Yu J. 2016. Autoinducer-2 of Streptococcus mitis as a Target Molecule to Inhibit Pathogenic Multi-Species Biofilm Formation In Vitro and in an Endotracheal Intubation Rat Model. Front Microbiol 7:88.

33. Li H, Li X, Wang Z, Fu Y, Ai Q, Dong Y, Yu J. 2015. Autoinducer-2 regulates Pseudomonas aeruginosa PAO1 biofilm formation and virulence production in a dose-dependent manner. BMC Microbiol 15:192.

34. Hardie KR, Heurlier K. 2008. Establishing bacterial communities by “word of mouth”: LuxS and autoinducer 2 in biofilm development. Nat Rev Microbiol 6:635–643.

35. Staphylococcus aureus autoinducer-2 quorum sensing decreases biofilm formation in an icaR -dependent manner | SpringerLink.

36. Hsiao A, Shamsir Ahmed AM, Subramanian S, Griffin NW, Drewry LL, Petri WA, Haque R, Ahmed T, Gordon JI. 2014. Members of the human gut microbiota involved in recovery from Vibrio cholerae infection. Nature 515:423–426.

37. Thompson JA, Oliveira RA, Djukovic A, Ubeda C, Xavier KB. 2015. Manipulation of the Quorum Sensing Signal AI-2 Affects the Antibiotic-Treated Gut Microbiota. Cell Rep 10:1861–1871.

38. Frontiers | AI-2 of Aggregatibacter actinomycetemcomitans inhibits Candida albicans biofilm formation | Cellular and Infection Microbiology.

39. Balestrino D, Haagensen JAJ, Rich C, Forestier C. 2005. Characterization of Type 2 Quorum Sensing in Klebsiella pneumoniae and Relationship with Biofilm Formation. J Bacteriol 187:2870–2880.

40. Sweeney EG, Nishida A, Weston A, Bañuelos MS, Potter K, Conery J, Guillemin K. 2019. Agent-Based Modeling Demonstrates How Local Chemotactic Behavior Can Shape Biofilm Architecture. mSphere 4.

41. Schlomann BH, Wiles TJ, Wall ES, Guillemin K, Parthasarathy R. 2018. Bacterial Cohesion Predicts Spatial Distribution in the Larval Zebrafish Intestine. Biophys J 115:2271–2277.

42. Wiles TJ, Jemielita M, Baker RP, Schlomann BH, Logan SL, Ganz J, Melancon E, Eisen JS, Guillemin K, Parthasarathy R. 2016. Host Gut Motility Promotes Competitive Exclusion within a Model Intestinal Microbiota. PLOS Biol 14:e1002517.

43. Schlomann BH, Wiles TJ, Wall ES, Guillemin K, Parthasarathy R. 2019. Sublethal antibiotics collapse gut bacterial populations by enhancing aggregation and expulsion. Proc Natl Acad Sci 116:21392–21400.

44. Wiles TJ, Schlomann BH, Wall ES, Betancourt R, Parthasarathy R, Guillemin K. 2020. Swimming motility of a gut bacterial symbiont promotes resistance to intestinal expulsion and enhances inflammation. PLOS Biol 18:e3000661.

45. Bivar Xavier K. 2018. Bacterial interspecies quorum sensing in the mammalian gut microbiota. C R Biol 341:297–299.

46. Laganenka L, Colin R, Sourjik V. 2016. Chemotaxis towards autoinducer 2 mediates autoaggregation in Escherichia coli. Nat Commun 7.

47. Jani S, Seely AL, V GLP, Jayaraman A, Manson MD. 2017. Chemotaxis to self-generated AI-2 promotes biofilm formation in Escherichia coli. Microbiology https://doi.org/10.1099/mic.0.000567.

48. Rolig AS, Mittge EK, Ganz J, Troll JV, Melancon E, Wiles TJ, Alligood K, Stephens WZ, Eisen JS, Guillemin K. 2017. The enteric nervous system promotes intestinal health by constraining microbiota composition. PLOS Biol 15:e2000689.

49. Xavier KB, Bassler BL. 2005. Regulation of Uptake and Processing of the Quorum-Sensing Autoinducer AI-2 in Escherichia coli. J Bacteriol 187:238–248.

50. Ismail AS, Valastyan JS, Bassler BL. 2016. A Host-Produced Autoinducer-2 Mimic Activates Bacterial Quorum Sensing. Cell Host Microbe 19:470–480.

51. Jemielita M, Taormina MJ, Burns AR, Hampton JS, Rolig AS, Guillemin K, Parthasarathy R. 2014. Spatial and Temporal Features of the Growth of a Bacterial Species Colonizing the Zebrafish Gut. mBio 5.

52. Stephens WZ, Burns AR, Stagaman K, Wong S, Rawls JF, Guillemin K, Bohannan BJM. 2016. The composition of the zebrafish intestinal microbial community varies across development. ISME J 10:644–654.

53. Bridges AA, Bassler BL. 2019. The intragenus and interspecies quorum-sensing autoinducers exert distinct control over Vibrio cholerae biofilm formation and dispersal. PLOS Biol 17:e3000429.

54. Westerfield M. 2007. The Zebrafish Book. A Guide for the Laboratory Use of Zebrafish (Danio Rerio), 5th ed. University of Oregon Press, Eugene, OR.

55. Melancon E, Gomez De La Torre Canny S, Sichel S, Kelly M, Wiles TJ, Rawls JF, Eisen JS, Guillemin K. 2017. Best practices for germ-free derivation and gnotobiotic zebrafish husbandry. Methods Cell Biol 138:61–100.

56. Datsenko KA, Wanner BL. 2000. One-step inactivation of chromosomal genes in Escherichia coli K-12 using PCR products. Proc Natl Acad Sci U S A 97:6640–6645.

57. Baba T, Ara T, Hasegawa M, Takai Y, Okumura Y, Baba M, Datsenko KA, Tomita M, Wanner BL, Mori H. 2006. Construction of Escherichia coli K-12 in-frame, single-gene knockout mutants: the Keio collection. Mol Syst Biol 2:2006.0008.

58. Murphy KC, Campellone KG. 2003. Lambda Red-mediated recombinogenic engineering of enterohemorrhagic and enteropathogenic E. coli. BMC Mol Biol 4:11.

59. Wiles TJ, Wall ES, Schlomann BH, Hay EA, Parthasarathy R, Guillemin K. 2018. Modernized Tools for Streamlined Genetic Manipulation and Comparative Study of Wild and Diverse Proteobacterial Lineages. mBio 9.

60. Milligan-Myhre K, Charette JR, Phennicie RT, Stephens WZ, Rawls JF, Guillemin K, Kim CH. 2011. Study of host-microbe interactions in zebrafish. Methods Cell Biol 105:87–116.

61. Chen X, Schauder S, Potier N, Van Dorsselaer A, Pelczer I, Bassler BL, Hughson FM. 2002. Structural identification of a bacterial quorum-sensing signal containing boron. 6871. Nature 415:545–549.

62. Ulrich DL, Kojetin D, Bassler BL, Cavanagh J, Loria JP. 2005. Solution Structure and Dynamics of LuxU from Vibrio harveyi, a Phosphotransferase Protein Involved in Bacterial Quorum Sensing. J Mol Biol 347:297–307.

63. Cámara M, Hardman A, Williams P, Milton D. 2002. Quorum sensing in *Vibrio cholerae*. Nat Genet 32:217–218.

64. Bainer R, Park H, Cluzel P. 2003. A high-throughput capillary assay for bacterial chemotaxis. J Microbiol Methods 55:315–319.

65. Pacheco AR, Sperandio V. 2009. Inter-kingdom signaling: chemical language between bacteria and host. Curr Opin Microbiol 12:192–198.

66. Karavolos MH, Winzer K, Williams P, Khan CMA. 2013. Pathogen espionage: multiple bacterial adrenergic sensors eavesdrop on host communication systems. Mol Microbiol 87:455–465.

67. Carey RM, Workman AD, Chen B, Adappa ND, Palmer JN, Kennedy DW, Lee RJ, Cohen NA. 2015. Staphylococcus aureus triggers nitric oxide production in human upper airway epithelium. Int Forum Allergy Rhinol 5:808–813.

68. Carey RM, Workman AD, Chen B, Adappa ND, Palmer JN, Kennedy DW, Lee RJ, Cohen NA. 2015. Staphylococcus aureus triggers nitric oxide production in human upper airway epithelium. Int Forum Allergy Rhinol 5:808–813.

69. Zargar A, Quan DN, Carter KK, Guo M, Sintim HO, Payne GF, Bentley WE. 2015. Bacterial Secretions of Nonpathogenic Escherichia coli Elicit Inflammatory Pathways: a Closer Investigation of Interkingdom Signaling. mBio 6.

70. Papenfort K, Bassler BL. 2016. Quorum sensing signal-response systems in Gram-negative bacteria. Nat Rev Microbiol 14:576–588.